

See discussions, stats, and author profiles for this publication at: <https://www.researchgate.net/publication/7604015>

Genetically Encoded Bright Ca²⁺ Probe Applicable for Dynamic Ca²⁺ Imaging of Dendritic Spines

ARTICLE *in* ANALYTICAL CHEMISTRY · OCTOBER 2005

Impact Factor: 5.64 · DOI: 10.1021/ac0506837 · Source: PubMed

CITATIONS

77

READS

53

5 AUTHORS, INCLUDING:



Masanori Matsuzaki

National Institute for Basic Biology

43 PUBLICATIONS 4,374 CITATIONS

SEE PROFILE



Junichi Nakai

Saitama University

48 PUBLICATIONS 2,127 CITATIONS

SEE PROFILE

Genetically Encoded Bright Ca^{2+} Probe Applicable for Dynamic Ca^{2+} Imaging of Dendritic Spines

Masamichi Ohkura,^{†,‡} Masanori Matsuzaki,[§] Haruo Kasai,^{§,||} Keiji Imoto,^{†,||} and Junichi Nakai^{*,†,||,⊥}

Department of Information Physiology, and Department of Cell Physiology, National Institute for Physiological Sciences, and School of Life Science, The Graduate University for Advanced Studies, Okazaki, Aichi 444-8585, Japan

G-CaMP is a Ca^{2+} probe based on a single green fluorescent protein (GFP). G-CaMP shows a large fluorescence increase upon Ca^{2+} binding, but its fluorescence is dim and pH sensitive, similar to other single GFP-based probes. Here we report an improved G-CaMP, named G-CaMP1.6, which enables easier detection of intracellular Ca^{2+} signals. G-CaMP1.6 was ~40 times more fluorescent than G-CaMP, mainly due to an increase in quantum yield. Furthermore, compared with G-CaMP, G-CaMP1.6 had not only a lower pH sensitivity but also a higher selectivity for divalent cations having an ionic radius similar to Ca^{2+} . Ca^{2+} sensitivity of G-CaMP1.6 ($K_d = 146$ nM, Hill coefficient = 3.8, $F_{\text{max}}/F_{\text{min}} = 4.9$) was slightly shifted toward higher affinity compared with that of G-CaMP. When expressed in mammalian cells, G-CaMP1.6 showed large fluorescence changes with drug applications. Notably, local Ca^{2+} changes in such tiny structures as dendritic spines of neurons were successfully observed with G-CaMP1.6, this being the first observation using a GFP-based probe. Additional mutations in Ca^{2+} -binding sites of G-CaMP1.6 shifted the affinity for Ca^{2+} and reduced the Ca^{2+} -buffering effect. G-CaMP1.6-CaM(E140K), which has a mutation in the Ca^{2+} binding site, is an improved probe with its increased brightness and reduced Ca^{2+} -buffering capacity.

Green fluorescent protein (GFP)¹ has been used as a component of fluorescent biosensors. One of the most remarkable merits of using protein-based biosensors is that they can be targeted to specific cells and intracellular organelles of interest by expressing their corresponding cDNAs with appropriate promoters or specific sequences encoding localization signals. GFP-based Ca^{2+} probes to date can be categorized into three groups, according to molecular mechanisms of reporting fluorescence signals: (1)

fluorescence resonance energy transfer (cameleons^{2–4} and FIP-CB_{SM},^{5,6} and TN-L15⁷), (2) chemiluminescence resonance energy transfer (GFP–aequorin fusion proteins⁸), and (3) conformational changes of GFP itself (camgaroos,^{9,10} G-CaMP,¹¹ and pericams¹²). Among them, the probes of the third group give large fluorescence changes. Taking this feature into consideration, we previously chose the strategy of the third group and developed a single GFP-based Ca^{2+} probe, named “G-CaMP”,¹¹ which is a fusion protein composed of a calmodulin (CaM) binding peptide M13, circularly permuted GFP, and CaM. G-CaMP shows a relatively large fluorescence change ($F_{\text{max}}/F_{\text{min}} = 4.5$) on Ca^{2+} binding and works at a submicromolar range of $[\text{Ca}^{2+}]_i$ ($K_d = 235$ nM). Recently, genetically engineered flies^{13–15} *C. elegans*,¹⁶ or mice¹⁷ expressing G-CaMP were developed, and fluorescence changes of G-CaMP have been successfully detected in their isolated tissues. Despite these practical benefits, G-CaMP has drawbacks as follows: (1) its fluorescence is dim, (2) it exhibits temperature-sensitive maturation, such that the probe is fluorescent at 28 °C but hardly fluorescent at 37 °C, (3) it requires several hours at 28 °C to become sufficiently fluorescent, (4) it is pH sensitive, and (5) it

- (2) Miyawaki, A.; Llopis, J.; Heim, R.; McCaffery, J. M.; Adams, J. A.; Ikura, M.; Tsien, R. Y. *Nature* **1997**, *388*, 882–887.
- (3) Miyawaki, A.; Griesbeck, O.; Heim, R.; Tsien, R. Y. *Proc. Natl. Acad. Sci. U.S.A.* **1999**, *96*, 2135–2140.
- (4) Nagai, T.; Yamada, S.; Tominaga, T.; Ichikawa, M.; Miyawaki, A. *Proc. Natl. Acad. Sci. U.S.A.* **2004**, *101*, 10554–10559.
- (5) Persechini, A.; Lynch, J. A.; Romoser, V. A. *Cell Calcium* **1997**, *22*, 209–216.
- (6) Romoser, V. A.; Hinkle, P. M.; Persechini, A. *J. Biol. Chem.* **1997**, *272*, 13270–13274.
- (7) Heim, N.; Griesbeck, O. *J. Biol. Chem.* **2004**, *279*, 14280–14286.
- (8) Baubet, V.; Le Mouellic, H.; Campbell, A. K.; Lucas-Meunier, E.; Fossier, P.; Brulet, P. *Proc. Natl. Acad. Sci. U.S.A.* **2000**, *97*, 7260–7265.
- (9) Baird, G. S.; Zacharias, D. A.; Tsien, R. Y. *Proc. Natl. Acad. Sci. U.S.A.* **1999**, *96*, 11241–11246.
- (10) Griesbeck, O.; Baird, G. S.; Campbell, R. E.; Zacharias, D. A.; Tsien, R. Y. *J. Biol. Chem.* **2001**, *276*, 29188–29194.
- (11) Nakai, J.; Ohkura, M.; Imoto, K. *Nat. Biotechnol.* **2001**, *19*, 137–141.
- (12) Nagai, T.; Sawano, A.; Park, E. S.; Miyawaki, A. *Proc. Natl. Acad. Sci. U.S.A.* **2001**, *98*, 3197–3202.
- (13) Wang, J. W.; Wong, A. M.; Flores, J.; Vossahl, L. B.; Axel, R. *Cell* **2003**, *112*, 271–282.
- (14) Suh, G. S.; Wong, A. M.; Hergarden, A. C.; Wang, J. W.; Simon, A. F.; Benzer, S.; Axel, R.; Anderson, D. J. *Nature* **2004**, *431*, 854–859.
- (15) Reiff, D. F.; Ihring, A.; Guerrero, G.; Isacoff, E. Y.; Joesch, M.; Nakai, J.; Borst, A. *J. Neurosci.* **2005**, *25*, 4766–4778.
- (16) Kahn-Kirby, A. H.; Dantzer, J. L.; Apicella, A. J.; Schafer, W. R.; Browne, J.; Bargmann, C. I.; Watts, J. L. *Cell* **2004**, *119*, 889–900.
- (17) Ji, G.; Feldman, M. E.; Deng, K. Y.; Greene, K. S.; Wilson, J.; Lee, J. C.; Johnston, R. C.; Rishniw, M.; Tallini, Y.; Zhang, J.; Wier, W. G.; Blaustein, M. P.; Xin, H. B.; Nakai, J.; Kotlikoff, M. I. *J. Biol. Chem.* **2004**, *279*, 21461–21468.

* Corresponding author. Phone: 81-48-462-1111 (Ext. 7559). Fax: 81-48-462-4697. E-mail: jnakai@brain.riken.jp.

[†] Department of Information Physiology, National Institute for Physiological Sciences.

[‡] Present address: First Department of Pharmacology, School of Pharmaceutical Sciences, Kyushu University of Health and Welfare, Yoshino, Nobeoka, Miyazaki 882-8508, Japan.

[§] Department of Cell Physiology, National Institute for Physiological Sciences.

^{||} School of Life Science, The Graduate University for Advanced Studies.

[⊥] Present address: Laboratory for Memory and Learning, RIKEN Brain Science Institute, Hirosawa, Wako, Saitama 351-0198, Japan.

(1) Prasher, D. C.; Eckenrode, V. K.; Ward, W. W.; Prendergast, F. G.; Cormier, M. J. *Gene* **1992**, *111*, 229–233.

presumably buffers as many as four Ca^{2+} ions per molecule. In the present work, we report cellular and subcellular Ca^{2+} measurements using an improved version of G-CaMP, named G-CaMP1.6. It is notable that G-CaMP1.6 enables easy measurements of Ca^{2+} changes in such tiny structures as dendritic spines of neurons.

EXPERIMENTAL SECTION

Materials. Restriction enzymes, modification enzymes, and ligases were purchased from New England Biolabs (Beverly, MA). pTriEx4neo vector was purchased from Biosciences Clontech (Palo Alto, CA). SuperFect and Ni-NTA were purchased from Qiagen (Hilden, Germany). FuGENE 6 was purchased from Roche (Basel, Switzerland). Fetal bovine serum, minimum essential medium, Hanks' balanced salt solution, and Pen-strep were purchased from Gibco (Tulsa, OK). Horse serum was purchased from Nichirei (Tokyo, Japan). Dulbecco's modified Eagle's medium and Trolox were purchased from Sigma-Aldrich (St. Louis, MO). Millicell culture insert was purchased from Millipore (Billerica, MA).

Plasmid Construction. The circularly permuted EGFP (cpEGFP149-144) used in this work was as reported previously.¹¹ For practical convenience, we created pN1-GCaMP1.3, in which the two *EcoRI* sites and the *HindIII* site in the CaM part of pN1-GCaMP¹¹ were destroyed by site-directed mutagenesis: GAATTC encoding Glu-11/Phe-12 was changed to GAATTT; GAAGCTTTC encoding Glu-14/Ala-15/Phe-16 to GAGGCTTTC; GAATTC encoding Glu-67/Phe-68 to GAGTTC (amino acid residue numbers described here correspond to those in CaM). In the cpEGFP part of pN1-GCaMP1.3, two amino acid changes of Val-163 to Ala (GCG) and Ser-175 to Gly (GGC) (amino acid residue numbers correspond to those in wild-type GFP) were made to yield pN1-GCaMP1.6. For bacterial expression of G-CaMP1.6 with a hexahistidine tag (His-6-tag), the 1.25-kb *BglIII*–*NotI* fragment of pN1-GCaMP1.6 was inserted into the 6.54-kb *BamHI*–*NotI* fragment of the pTriEx4neo vector, resulting in pTriEx4neo-GCaMP1.6. pN1-4neo-GCaMP1.6, which enabled mammalian expression of G-CaMP1.6 with the His-6-tag, was also constructed as follows: the cDNA sequence for the His-6-tagged G-CaMP1.6 was amplified by polymerase chain reaction (PCR) using pTriEx4neo-GCaMP1.6 as a template; the PCR primers used were 5'-AATGGATCCGC-CACCATGGCACACCATCACCACCATCAC-3' (forward) and 5'-GCGCGGCCGCTCATTCTCGCTGTCATCATTTGTAC-3' (reverse); the 1.45-kb PCR product was digested with *BamHI* and *NotI* and ligated to the 3.94-kb *BglIII*–*NotI* fragment of the pEGFP-N1 vector (Clontech, Palo Alto, CA). Amino acid changes from Glu to Lys at residues 31, 67, 104, and 140 (corresponding amino acid numbers are those in CaM) in the CaM part of pN1-4neo-GCaMP1.6 were also performed by PCR as follows: for Glu-31 to Lys, AAGCTT (*HindIII* site) was created to encode Lys-31/Leu-32; for Glu-67 to Lys, GAA encoding Glu-67 was replaced with AAA together with the introduction of a *PvuI* site at ACAATCGAC encoding Thr-62/Ile-63/Asp-64 by replacing with ACGATCGAC; for Glu-104 to Lys, AAGCTT (*HindIII* site) was created to encode Lys-104/Leu-105; for Glu-140 to Lys, GAG encoding Glu-140 was changed to AAG. To prepare EGFP used as a standard protein in in vitro fluorescence measurements, pTriEx4neo-His₆EGFP was constructed as follows: the cDNA sequence for EGFP was amplified by PCR using pEGFP-N1 as a template; the PCR primers

used were 5'-GGCCATGGCACACCATCACCACCATCACGGA-GATCTAAGCAAGGGCGAGGAGCTGTTC-3' (forward) and 5'-GCGAATTCGGATCCGCGGCCGCTTACTTGTACAGCTCGTC-CAT-3' (reverse); the 0.74-kb PCR product was digested with *NcoI* and *NotI* and ligated to the 6.36-kb *NcoI*–*NotI* fragment of the pTriEx4neo vector. All the constructs described above were verified by DNA sequencing.

Bacterial Expression and in Vitro Spectroscopic Measurements. Recombinant fluorescent proteins with the His-6-tag at the N-terminus were expressed in *Escherichia coli* BL21(DE3)-pLysS at 28 °C, purified by Ni-NTA, and spectroscopically characterized as described previously.¹¹ pH titrations were performed by using a series of buffers prepared with pHs ranging from 5.5 to 10, and Ca^{2+} titrations were performed by cumulative additions of CaCl_2 in the presence of 20 mM BAPTA, 100 mM KCl, and 20 mM MOPS (pH 7.5) as described.¹¹ Cl^- titrations for G-CaMP variants were carried out at 0.3 μM protein concentrations by fluorescence spectroscopy excited at 470 nm and monitored at 510 nm in buffers containing various concentrations of KCl (10, 50, 100, and 200 mM), where total concentrations of K^+ were constant at 200 mM using potassium gluconate and 20 mM MOPS (pH 7.5) with 5 mM EGTA or 100 μM Ca^{2+} . To test effects of divalent cations (Ni^{2+} , Mg^{2+} , Co^{2+} , Zn^{2+} , Mn^{2+} , Cd^{2+} , Sr^{2+} , and Ba^{2+} ; all chloride salts except NiSO_4) on fluorescence changes of G-CaMP variants (at 0.3 μM protein concentrations in KM buffer containing 100 mM KCl and 20 mM MOPS (pH 7.5)), the ratio $(F_{\text{cation}} - F_{\text{EDTA}})/F_{\text{EDTA}}$ was calculated and normalized to that for Ca^{2+} of 1.0, where F_{EDTA} was the initial fluorescence intensity in the presence of 1 mM EDTA and F_{cation} was the fluorescence intensity after the addition of 2 mM divalent cation measured by fluorescence spectroscopy excited at 470 nm and monitored at 510 nm. Fluorescence or absorbance change of G-CaMP1.6 following the temperature shift from 28 to 37 °C was examined as follows: Purified G-CaMP1.6 protein (at 3 μM protein concentration in KM buffer with 5 mM EGTA) was incubated at 28 °C for 20 h before starting measurements. After the initial measurement (for fluorescence, excited at 470 nm and monitored at 510 nm) at 28 °C, samples were moved to a 37 °C incubator for appropriate periods and subjected to measurements. Total time required for each measurement was ~ 1 min.

Measurements of Extinction Coefficient (ϵ) and Quantum Yield (Φ). These values were determined by comparison to EGFP ($\epsilon = 56000$, $\Phi = 0.60$) as a standard as described.¹⁸ Absorbance and fluorescence emission spectra were measured in the KM buffer. Protein concentrations were measured by the Bradford method¹⁹ with bovine serum albumin as a standard protein.

$^{45}\text{Ca}^{2+}$ Overlay. CaM variants of G-CaMP1.6 (100 pmol each) were blotted onto nitrocellulose membranes and incubated for 1 h at room temperature with the KM buffer including 500 μM $^{45}\text{CaCl}_2$ (100 kBq/mL). Then the membranes were washed for 10 min with 50% ethanol twice and air-dried. The remaining radioactivity on the membranes was measured using an image analyzer BAS-5000 (Fuji Film, Tokyo, Japan).

Fluorescence Measurements in HEK293 and PC12 Cells. HEK293 and PC12 cells were cultured in growth medium

(18) Ward, W. W. In *Green Fluorescent Protein: Properties, Applications, and Protocols*; Chalfie, M., Kain, S., Eds.; John Wiley & Sons: New York, 1997; pp 45–75.

(19) Bradford, M. M. *Anal. Biochem.* **1976**, *72*, 248–254.

composed of Dulbecco's modified Eagle's medium and 10% fetal bovine serum and transfected with plasmids by using SuperFect or FuGENE 6 according to the manufacturer's manuals. Transfected HEK293 and PC12 cells were incubated at 37 °C for 1–4 days and then at 28 °C for overnight before testing. Images for G-CaMP1.6 and its CaM mutant (E140K), named G-CaMP1.6-CaM(E140K), were recorded with a fluorescence microscope (IX70, Olympus, Tokyo, Japan) equipped with a CCD camera (ORCA-ER, Hamamatsu Photonics, Hamamatsu, Japan) and analyzed by using the AquaCosmos version 1.3 software (Hamamatsu Photonics). The excitation filter, the dichroic mirror, and the emission filter used were BP470-490, DM505, and BA515-550, respectively (All from Olympus). To test the time course of G-CaMP and G-CaMP1.6 fluorescence development, HEK293 cells were transfected with the same amount of plasmids (1 μ g/3.5-cm dish) and cultured at 37 °C for 2 days. After exchanging culture media with HEPES-buffered saline (HBS) containing 107 mM NaCl, 6 mM KCl, 1.2 mM MgSO₄, 2 mM CaCl₂, 1.2 mM KH₂PO₄, 11.5 mM glucose, and 20 mM HEPES (pH 7.4),²⁰ which was prewarmed to 37 °C, cells were preincubated for another 30 min at 37 °C, immediately moved to the microscope stage, and tested. Total time required to set the transfected cells to the microscope stage prior to starting the measurement (time 0) was ~2 min. Intervals between acquired images for G-CaMP1.6 and G-CaMP were 2 and 10 min, respectively. After each measurement, successfully transfected cells were obviously fluorescent and their averaged fluorescence intensities were analyzed after subtraction of background fluorescence. To measure fluorescence of G-CaMP variants, transfected HEK293 or PC12 cells were perfused with HBS at room temperature, and 100 μ M carbachol for HEK293 cells or 100 μ M ATP for PC12 cells was applied to the bath, followed by applications of 5 μ M ionomycin with and without 10 mM EDTA as described previously.¹¹ Intracellular pH (pH_i) was measured at room temperature with a confocal laser scanning microscope (TCS SP2, Leica, Wetzlar, Germany). In brief, the cells loaded with 5 μ M BCECF-AM were perfused with HBS, and the drugs tested in fluorescence measurements of G-CaMP variants were applied to the bath. Fluorescence images sequentially excited at 458 and 488 nm were monitored at 480–510 and 510–550 nm, respectively. Images were taken at 5-s intervals. pH_i calibration was done using 5 μ M carbonyl cyanide 4-(trifluoromethoxy)-phenylhydrazone dissolved in HBS with pH adjusted to 4.0, 7.4, and 9.0 as described previously.²¹

Hippocampal Slice Experiments. Rat hippocampal slices were obtained as described previously.²² The animal experiments were approved by the animal experiment committee of the National Institute for Physiological Sciences, Japan. In brief, hippocampal slices with a thickness of 350 μ m were obtained from P6 Sprague–Dawley rats and incubated on Millicell culture inserts in 5% CO₂ at 35 °C. Culture medium was composed of 50% minimum essential medium, 25% Hanks balanced salt solution, 25% horse serum, 6.5 g/L glucose, and 1% Pen-strep. Slices cultured for 5 days were transfected by using biolistic particle-

mediated delivery (PDS-1000, Bio-Rad, Hercules, CA) with 1.6- μ m gold particles coated with pN1-4neo-GCaMP1.6. Slices were cultured at 35 °C for additional 5 days after transfection. A slice was transferred to a recording chamber, which was superfused with a solution containing 125 mM NaCl, 2.5 mM KCl, 1 mM MgCl₂, 2 mM CaCl₂, 1.25 mM NaH₂PO₄, 26 mM NaHCO₃, 20 mM glucose, 1 μ M tetrodotoxin, 50 μ M picrotoxin, and 200 μ M Trolox bubbled with 95% O₂ and 5% CO₂. Experiments were started ~30 min after the slice was set to the recording chamber kept at room temperature (23–25 °C). Two-photon excitation imaging of neurons was performed with an upright microscope (BX50, Olympus) equipped with a water immersion objective lens (LUMPlanFI/IR 60x, numerical aperture, 0.9) as described previously.²³ Mode-locked femtosecond-pulse Ti:sapphire laser (Tsunami, Spectra Physics, Mountain View, CA) tuned to 910-nm wavelength was attached to a laser-scanning microscope (FluoView, Olympus). Images were acquired and analyzed with the FluoView software. In the fluorescence measurements, 100 μ M glutamate was applied by puff. During the glutamate application, there may be some fluorescence change due to intracellular acidification. However, it should be negligible in this experiment, because (1) the duration of the glutamate application was only 6.5 s and this is too short to make a big pH change, and (2) when cells become acidic, fluorescence intensity of the probe should decrease (see Figure 2C) and this was not our case.

RESULTS

Modification of G-CaMP. The original G-CaMP is a single GFP-based Ca²⁺ probe, in which a CaM-binding peptide M13, cpEGFP, and CaM are connected in tandem in this order from the N- to the C-terminus. When Ca²⁺ ions bind to the CaM EF hands, subsequent Ca²⁺–CaM–M13 interaction induces conformational changes in the cpEGFP part, resulting in an increase in chromophore fluorescence. G-CaMP has the favorable feature of a relatively large (~4.5-fold) increase in fluorescence intensity in response to Ca²⁺ binding. However, it has several limitations: the fluorescence of the probe is dim, the probe is hardly fluorescent at 37 °C because of its temperature sensitivity, and it takes several hours to become sufficiently fluorescent even at lower temperatures.¹¹ Aiming at creation of a G-CaMP version with bright fluorescence and stability at 37 °C, we introduced amino acid replacements of Val-163 with Ala (V163A) and Ser-175 with Gly (S175G), which were known to provide more efficient chromophore formation of GFP,²⁴ in the cpEGFP part of G-CaMP, and developed a G-CaMP version named G-CaMP1.6. With a His-6-tag attached at the N-terminus, this new probe was expressed in *E. coli* at 28 °C and purified by using a Ni column. Purified G-CaMP1.6 was more brightly fluorescent than G-CaMP at a same concentration.

Figure 1A and B, respectively, shows absorbance spectra of purified G-CaMP and G-CaMP1.6 in the absence and the presence of Ca²⁺. In the absence of Ca²⁺, both the original and modified G-CaMPs had two absorbance peaks at 400–410 and ~490 nm. Their absorbance spectra were similar to that of wild-type GFP.²⁴ Therefore, these absorbance peaks may correspond to the neutralized (protonated 400–410-nm peak) and ionized (depro-

(20) Okada, T.; Inoue, R.; Yamazaki, K.; Maeda, A.; Kurosaki, T.; Yamakuni, T.; Tanaka, I.; Shimizu, S.; Ikenaka, K.; Imoto, K.; Mori, Y. *J. Biol. Chem.* **1999**, *274*, 27359–27370.

(21) James-Kracke, M. R. *J. Cell. Physiol.* **1992**, *151*, 596–603.

(22) Matsuzaki, M.; Ellis-Davies, G. C. R.; Nemoto, T.; Miyashita, Y.; Iino, M.; Kasai, H. *Nat. Neurosci.* **2001**, *4*, 1086–1092.

(23) Nemoto, T.; Kimura, R.; Ito, K.; Tachikawa, A.; Miyashita, Y.; Iino, M.; Kasai, H. *Nat. Cell Biol.* **2001**, *3*, 253–258.

(24) Tsien, R. Y. *Annu. Rev. Biochem.* **1998**, *67*, 509–544.

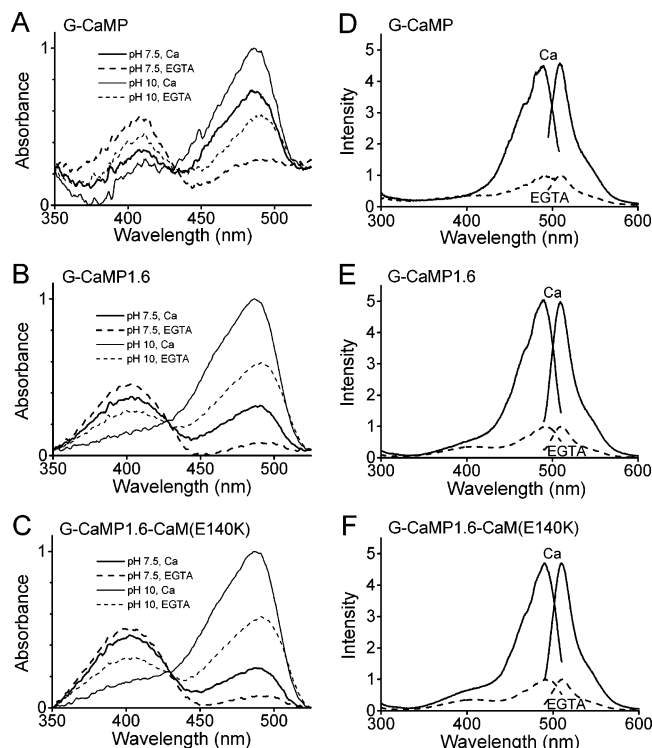


Figure 1. Spectral properties of G-CaMP, G-CaMP1.6, and G-CaMP1.6-CaM(E140K). (A–C) Absorbance spectra were obtained at pH 7.5 (thick lines) or pH 10 (thin lines) in the presence of 100 μM Ca^{2+} (solid lines) or 5 mM EGTA (broken lines) and were normalized to a maximum value of 1.0. (D–F) Excitation spectra detected at 520 nm and emission spectra excited at 470 nm were obtained at pH 7.5 in the presence of 100 μM Ca^{2+} (solid lines) or 5 mM EGTA (broken lines) and were normalized to a maximum value in the presence of EGTA of 1.0.

Table 1. Characterizations of G-CaMP and Its Variants

name	Ca^{2+}	λ_{abs}^a (nm)	λ_{em}^c (nm)	$\text{p}K_a^e$ (pH)
G-CaMP	–	409 (1100)		
	+	488 (570)	510 (0.03)	8.1 (0.84)
	+	410 (690)		
G-CaMP1.6	–	487 (1400)	510 (0.05)	7.1 (0.82)
	+	489 (1100)	510 (0.56)	8.8 (0.70)
	+	403 (5200)		
G-CaMP1.6-CaM(E140K)	–	488 (3800)	509 (0.79)	8.2 (0.54)
	+	404 (6000)		
	+	491 (1200)	511 (0.30)	8.6 (0.63)
	+	403 (5400)		
	+	490 (3100)	510 (0.54)	8.7 (0.69)

^a Absorbance peak (nm). ^b Extinction coefficient ($\text{M}^{-1}\text{cm}^{-1}$). ^c Emission peak (nm). ^d Quantum yield. ^e Obtained from three independent measurements. ^f Hill coefficient for proton.

tonated 490-nm peak) forms of the chromophore. With excess amount of Ca^{2+} , the 490-nm absorbance peak increased at the expense of the 400-nm peak, suggesting that chromophores of G-CaMP and G-CaMP1.6 became more ionized when Ca^{2+} bound to the CaM part of probes. The extinction coefficients (ϵ) at 490 nm of G-CaMP1.6 were 1.9 and 2.7 times higher in the absence and the presence of Ca^{2+} , respectively, than those of G-CaMP (Table 1).

Fluorescence excitation and emission spectra of G-CaMP and G-CaMP1.6 in the absence and the presence of Ca^{2+} are shown

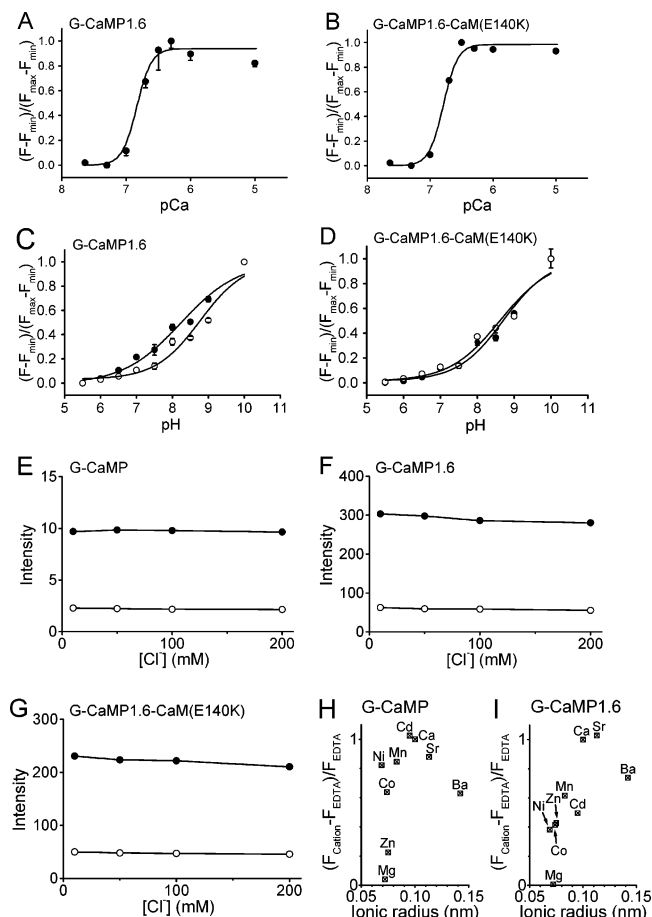


Figure 2. Comparisons of in vitro properties among G-CaMP1.6, G-CaMP1.6-CaM(E140K), and G-CaMP. Ca^{2+} titration curves at pH 7.5 for G-CaMP1.6 (A) and G-CaMP1.6-CaM(E140K) (B) are shown. pH titration curves for G-CaMP1.6 (C) and G-CaMP1.6-CaM(E140K) (D) were obtained in the presence of 100 μM Ca^{2+} (●) or 5 mM EGTA (○). (C and D) Fluorescence ratios were normalized so that maximum fluorescence ratios corresponded to 1.0. At pH 10, fluorescence intensities with Ca^{2+} of G-CaMP, G-CaMP1.6, and G-CaMP1.6-CaM(E140K) were 1.6, 1.6, and 1.9 times larger, respectively, than those with EGTA (data not shown). (A–D) Data points represent means with standard deviations of three independent experiments. Cl^- titration curves for G-CaMP (E), G-CaMP1.6 (F), and G-CaMP1.6-CaM(E140K) (G) were obtained in the presence of 100 μM Ca^{2+} (●) or 5 mM EGTA (○) at pH 7.5. Relationships between ionic radii of divalent cations and their effects on fluorescence changes for G-CaMP (H) and G-CaMP1.6 (I) were analyzed at pH 7.5. ($F_{\text{cation}} - F_{\text{EDTA}}/F_{\text{EDTA}}$) for tested cations are plotted as a function of their ionic radii^{25,26} after normalization to that for Ca^{2+} of 1.0.

in Figure 1D and E, respectively. Although Ca^{2+} shifted only a little, the excitation and the emission spectra for either G-CaMP or G-CaMP1.6 (at most ~ 1 -nm shift each; Table 1), it markedly enhanced the fluorescence intensities of both probes. Maximum fluorescence change upon Ca^{2+} binding ($F_{\text{max}}/F_{\text{min}}$) for G-CaMP1.6 was 4.9, which was sufficiently large, and even larger than that for G-CaMP ($F_{\text{max}}/F_{\text{min}} = 4.5$). The quantum yields (Φ) at 510 nm of G-CaMP1.6 were 19 times larger in the absence of Ca^{2+} and 16 times larger in the presence of Ca^{2+} than those of G-CaMP (Table 1). Because brightness is proportional to the product of extinction coefficient and quantum yield, G-CaMP1.6 is ~ 40 times more fluorescent than G-CaMP.

Figure 2A shows a Ca^{2+} titration curve of G-CaMP1.6 fluorescence, which was fitted with the Hill equation, revealing an

apparent K_d for Ca^{2+} of 146 nM and a Hill coefficient of 3.8. The apparent K_d value was slightly lower than that of G-CaMP (235 nM).¹¹ Figure 2C illustrates the pH sensitivity of G-CaMP1.6 fluorescence. The apparent pK_a value of G-CaMP1.6 was 8.8 or 8.2 in the absence or the presence of Ca^{2+} , respectively, showing a slight alkaline shift of the pH titration curve compared with G-CaMP¹¹ (Table 1). Moreover, it is notable that the Hill coefficients for proton of G-CaMP1.6 were smaller than those of G-CaMP in the absence or the presence of Ca^{2+} (Table 1). This result demonstrates a reduced pH sensitivity of G-CaMP1.6 in comparison with G-CaMP.

It has been reported that some GFP variants are also sensitive to halides.²⁴ As shown in Figure 2E and F, fluorescence intensity for both G-CaMP and G-CaMP1.6 was insensitive to Cl^- regardless of the presence of 100 μM Ca^{2+} or 5 mM EDTA. In addition, because several divalent cations similar to Ca^{2+} in ionic radius (0.100 nm) were reported to cause conformational changes of CaM at submillimolar concentrations²⁵ and to affect the CaM–M13 interaction,²⁶ we investigated effects of divalent cations on fluorescence changes of G-CaMP variants. Among the divalent cations tested (Ni^{2+} , Mg^{2+} , Co^{2+} , Zn^{2+} , Mn^{2+} , Cd^{2+} , Sr^{2+} , and Ba^{2+} at 1 mM each as free cations), all except Mg^{2+} caused increases in fluorescence intensity of both G-CaMP and G-CaMP1.6 (Figure 2H and I). Mg^{2+} was not only inactive by itself but also unable to antagonize Ca^{2+} -induced fluorescence increases for either G-CaMP or G-CaMP1.6 (data not shown). Ba^{2+} and Sr^{2+} , which are sometimes used as carrier ions for electrophysiological experiments, showed fairly large fluorescence increases at 1 mM, but their affinities were much lower than that of Ca^{2+} (K_d values for Ba^{2+} and Sr^{2+} were 260 and 370 μM for G-CaMP and 80 and 460 μM for G-CaMP1.6). Although we expected that Ni^{2+} and Co^{2+} (their ionic radii are 0.069 and 0.074 nm, respectively)²⁶ should be ineffective or much less effective, based on the fact that they had little effect on conformational changes of CaM²⁵ and Ca^{2+} –CaM–M13 interactions,²⁶ our results indicated that they significantly increased fluorescence intensity of G-CaMP variants. Another interesting observation was that divalent cations that strongly increased fluorescence intensity ($F_{\text{cation}} - F_{\text{EDTA}})/F_{\text{EDTA}}$ were different even between G-CaMP and G-CaMP1.6. The divalent cations that showed normalized $(F_{\text{cation}} - F_{\text{EDTA}})/F_{\text{EDTA}} > 0.8$ for G-CaMP were Ni^{2+} , Mn^{2+} , Cd^{2+} , Ca^{2+} , and Sr^{2+} , whereas those for G-CaMP1.6 were only Ca^{2+} and Sr^{2+} . This result also demonstrates that G-CaMP1.6 has a higher selectivity than G-CaMP to divalent cations having an ionic radius similar to Ca^{2+} .

Time Course for the Temperature-Dependent Fluorescence Change of G-CaMP1.6. Although G-CaMP1.6 was hardly fluorescent at 37 °C when expressed in cells, an obvious improvement of G-CaMP1.6 over G-CaMP was its brightness and faster time course to reach a sufficient fluorescence level at 28 °C. Figure 3A and B shows the time course for fluorescence increases of G-CaMP1.6 and G-CaMP following the temperature change from 37 to 28 °C. As shown in Figure 3A, the fluorescence increase at 120 min for G-CaMP1.6 was ~32 times larger than that for G-CaMP. Although it is known that even a single amino acid replacement sometimes influences protein production, degrada-

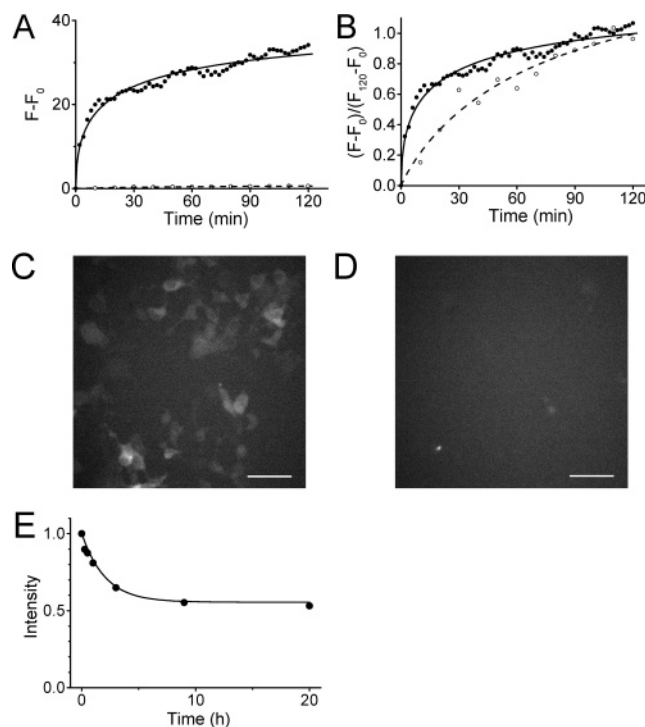


Figure 3. Temperature-dependent fluorescence change for G-CaMP1.6. (A–D) Time course of fluorescence increases due to the temperature shift from 37 to 28 °C for HEK293 cells expressing G-CaMP1.6 and G-CaMP. Data for G-CaMP1.6 (●) and G-CaMP (○) were fitted according to single-exponential equations (solid lines for G-CaMP1.6 and broken lines for G-CaMP). F_0 , F_{120} , and F were fluorescence intensities at 0 min, at 120 min, and at a time between 0 and 120 min, respectively. (A) Fluorescence increase at each time point ($F - F_0$) is plotted. (B) Fluorescence increase at each time point ($F - F_0$) was normalized to that at 120 min ($F_{120} - F_0$) of 1.0. The time constant of fluorescence increase for G-CaMP1.6 was 22 min, while that for G-CaMP was 77 min. Fluorescence images of G-CaMP1.6 (C) and G-CaMP (D) are shown at 30 min. Scale bars indicate 100 μm . (E) Time course of fluorescence decrease for the purified G-CaMP1.6 protein due to the temperature shift from 28 to 37 °C under a Ca^{2+} -free condition. Data are fitted according to single-exponential equations. Fluorescence intensity at each time point was normalized to that at 0 min of 1.0. The time constant of fluorescence decrease was 122 min.

tion, or both in cells, the fluorescence difference between G-CaMP1.6 and G-CaMP was considered mainly due to their own brightness (extinction coefficients and quantum yields) rather than their expression levels in cells, because average fluorescence intensities measured from many cells were compared. Furthermore, the fluorescence difference between G-CaMP1.6 and G-CaMP (~32 times) was in agreement with that observed between purified G-CaMP1.6 and G-CaMP in the spectroscopic analysis; i.e., purified G-CaMP1.6 was ~36 times more fluorescent than G-CaMP in the absence of Ca^{2+} (Table 1). To compare the speed of fluorescence development by the temperature change from 37 to 28 °C for G-CaMP1.6 with that for G-CaMP, each time course of fluorescence increase normalized to the value at 120 min was plotted (Figure 3B). The time constant of fluorescence increases was 22 min for G-CaMP1.6 and 77 min for G-CaMP, respectively, indicating that the fluorescence development of G-CaMP1.6 was ~3.5 times faster than that of G-CaMP. Quick development of fluorescence is important from a practical point of view. In fact, at 30 min after lowering the temperature from 37 to 28 °C, the

(25) Chao, S. H.; Suzuki, Y.; Zysk, J. R.; Cheung, W. Y. *Mol. Pharmacol.* **1984**, 26, 75–82.

(26) Ozawa, T.; Sasaki, K.; Umezawa, Y. *Biochim. Biophys. Acta* **1999**, 1434, 211–220.

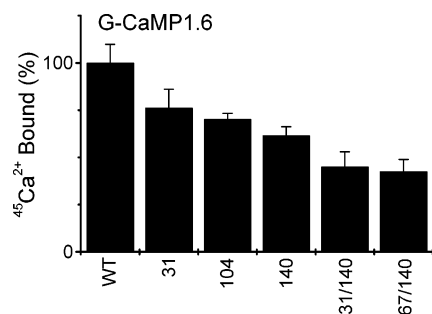


Figure 4. Comparisons of Ca^{2+} binding among several CaM mutants of G-CaMP1.6. $^{45}\text{Ca}^{2+}$ bound to CaM mutants of G-CaMP1.6 is shown after normalization to that for G-CaMP1.6 of 100%. Data points represent means with standard deviations of three independent experiments.

fluorescence image of G-CaMP1.6 was more frequently captured than that of G-CaMP (Figure 3C and D). Conversely, once G-CaMP1.6 became fluorescent at 28 °C, it stayed fluorescent more than 1 day even at 37 °C (data not shown).

We next heated the purified G-CaMP1.6 protein in order to know how stable G-CaMP1.6 is at 37 °C. For this purpose, we measured the absorbance and the fluorescence of the purified G-CaMP1.6 at 28 °C and then at 37 °C. Fluorescence intensity of the purified G-CaMP1.6 decreased to 53% of the initial fluorescence intensity at 20 h after shifting temperature from 28 to 37 °C under a Ca^{2+} -free condition (time constant 2.0 h) (Figure 3E). This fluorescence decrease was not due to the damage of the chromophore, because this process is reversible and fluorescence came back when the temperature was shifted from 37 to 28 °C (data not shown). Surprisingly, there was little difference between the absorbance of G-CaMP1.6 at these temperatures during this period (data not shown). This result suggests that the chromophore stability of G-CaMP1.6 may be temperature-independent in physiological temperature range and that the temperature dependence for the brightness of G-CaMP1.6 may be mainly derived from the change in quantum yield.

Effect of Disrupting Each EF Hand of CaM in G-CaMP1.6.

Since the Ca^{2+} -sensing of G-CaMP or its variants is attributable to Ca^{2+} binding to the four EF hands²⁷ of the CaM part of the probes, amino acid replacement at each EF hand should reduce the affinity for Ca^{2+} and reduce the number of Ca^{2+} ions that bind to the probes (Ca^{2+} -buffering effect). Because it has been reported that amino acid replacements of glutamate (E) with lysine (K) at CaM amino acid residue positions of 31, 67, 104, and 140 (E31K, E67K, E104K, and E140K, respectively) significantly impair Ca^{2+} binding to CaM at respective EF hands,^{28,29} these mutations were introduced in G-CaMP1.6. As expected, the tested G-CaMP1.6 variants with one or two EF hand mutations in the CaM part showed reasonably reduced $^{45}\text{Ca}^{2+}$ binding (Figure 4). However, we could not make a CaM mutant with the dramatically altered affinity for Ca^{2+} (Table 2). On the other hand, there was a tendency that the fluorescence change ($F_{\text{max}}/F_{\text{min}}$) decreased when more EF hands were disrupted (Table 2). Among the CaM

Table 2. Ca^{2+} Sensitivity of G-CaMP and Its Variants

name	Ca^{2+} sensitivity ^a		
	K_d (nM)	Hill coeff	$F_{\text{max}}/F_{\text{min}}$ ^b
G-CaMP	235	3.3	4.5
G-CaMP1.6	146	3.8	4.9
G-CaMP1.6–CaM(E31K)	159	3.4	3.2
G-CaMP1.6–CaM(E67K)	nd ^c	nd	1.7
G-CaMP1.6–CaM(E104K)	205	4.2	4.3
G-CaMP1.6–CaM(E140K)	161	3.9	4.7
G-CaMP1.6–CaM(E31K/E67K)	nd	nd	1.5
G-CaMP1.6–CaM(E31K/E104K)	nd	nd	1.5
G-CaMP1.6–CaM(E31K/E140K)	330	2.2	2.7
G-CaMP1.6–CaM(E67K/E104K)	nd	nd	1.0
G-CaMP1.6–CaM(E67K/E140K)	242	1.4	1.9
G-CaMP1.6–CaM(E104K/E140K)	nd	nd	1.0

^a Obtained from three independent measurements. ^b The peak fluorescence intensity at 510 nm with Ca^{2+} (F_{max}) was divided by that with EGTA (F_{min}). ^c nd, not determined because of the presence of two or more different affinities for Ca^{2+} .

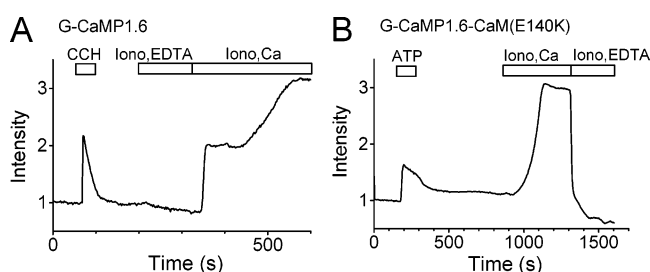


Figure 5. Typical fluorescence changes in mammalian cells monitored with G-CaMP1.6 and G-CaMP1.6–CaM(E140K). G-CaMP1.6 (A) and G-CaMP1.6–CaM(E140K) (B) were expressed in HEK293 and PC12 cells, respectively. Applications of 100 μM carbachol (CCH), 100 μM ATP, or 5 μM ionomycin (Iono) with and without Ca^{2+} are indicated by open boxes.

mutants tested, G-CaMP1.6–CaM(E140K) possessed similar Ca^{2+} sensitivity ($K_d = 161$ nM, Hill coefficient 3.9) and fluorescence change ($F_{\text{max}}/F_{\text{min}} = 4.7$), compared with G-CaMP1.6 (Figures 1C,F and 2B,D,G). Since G-CaMP1.6–CaM(E140K) buffers less Ca^{2+} than G-CaMP1.6 (Figure 4), G-CaMP1.6–CaM(E140K) is a better Ca^{2+} probe than G-CaMP1.6 for monitoring $[\text{Ca}^{2+}]_i$ when applied in cells.

Application of G-CaMP Variants to Mammalian Cells. We

next tested G-CaMP1.6 and G-CaMP1.6–CaM(E140K) in HEK293 and PC12 cells, in which Ca^{2+} transients were evoked by stimulation of endogenous muscarinic and purinergic receptors, respectively. The stimulation of the muscarinic receptors in HEK293 cells by carbachol causes the increase of $[\text{Ca}^{2+}]_i$ due to the Ca^{2+} release from the endoplasmic reticulum,³⁰ while the stimulation of the purinergic receptors in PC12 cells by ATP causes both the Ca^{2+} release and the Ca^{2+} influx from the extracellular space.³¹ Figure 5A illustrates that application of 100 μM carbachol elicited a large increase in fluorescence in HEK293 cell expressing G-CaMP1.6. Figure 5B demonstrates that G-CaMP1.6–CaM(E140K) showed a fluorescence increase during application of 100 μM ATP in PC12 cells. Neither G-CaMP1.6 nor

(27) Kretsinger, R. H.; Nockolds, C. E. *J. Biol. Chem.* **1973**, *248*, 3313–3326.

(28) Maune, J. F.; Klee, C. B.; Beckingham, K. *J. Biol. Chem.* **1992**, *267*, 5286–5295.

(29) Gao, Z. H.; Krebs, J.; VanBerkum, M. F.; Tang, W. J.; Maune, J. F.; Means, A. R.; Stull, J. T.; Beckingham, K. *J. Biol. Chem.* **1993**, *268*, 20096–20104.

(30) Bischof, G.; Serwold, T. F.; Machen, T. E. *Cell Calcium* **1997**, *21*, 135–142.

(31) Barry, V.; Cheek, T. *J. Cell Sci.* **1994**, *107*, 451–462.

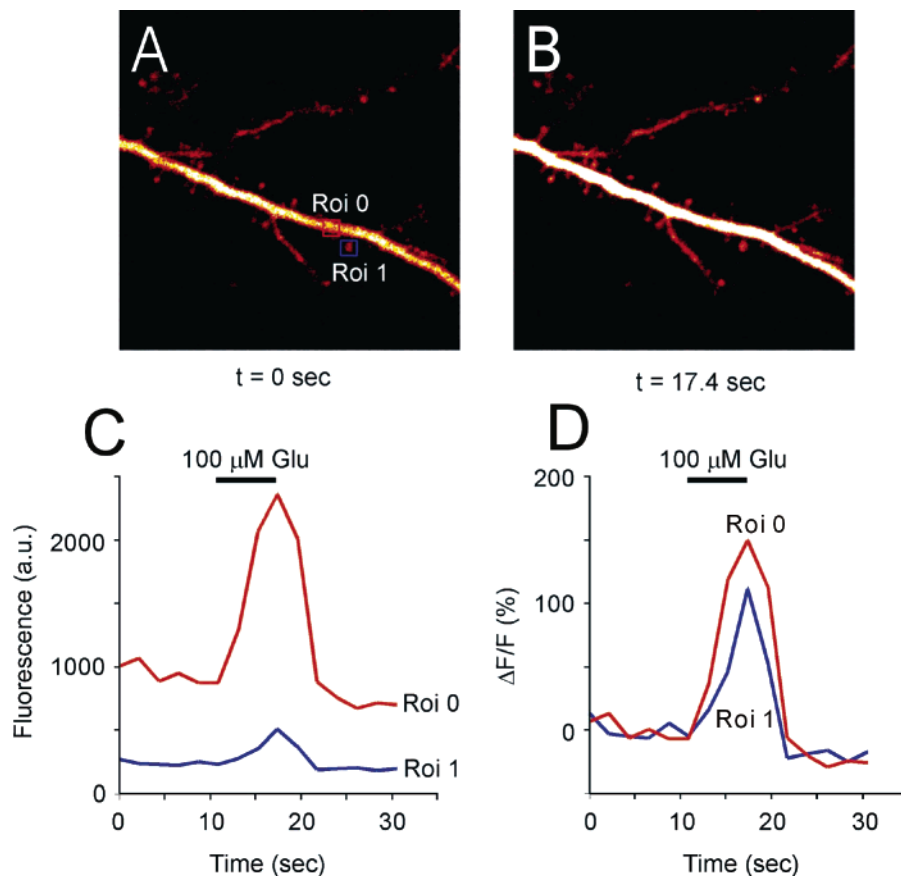


Figure 6. Measurement of fluorescence changes in rat hippocampal CA1 neuron monitored with G-CaMP1.6. Fluorescence images were taken before ($t = 0$ s) (A) and after ($t = 17.4$ s) (B) application of $100 \mu\text{M}$ glutamate (Glu). (C) Fluorescence intensities at a dendritic shaft (Roi 0) and a dendritic spine (Roi 1) in (A) are plotted. (D) Fluorescence increase at each time point (ΔF) was normalized to fluorescence intensity obtained immediately before application of Glu (F) of 100%. Red line and blue line show $\Delta F/F$ obtained at Roi 0 and Roi 1, respectively.

G-CaMP1.6–CaM(E140K) exhibited photoisomerization.^{11,32} Therefore, these G-CaMP variants proved to be excellent Ca^{2+} probes in mammalian cells. In parallel experiments, we monitored pH_i during carbachol or ATP application to observe no change in pH_i (7.3 and 7.7 in HEK293 and PC12 cells, respectively; data not shown), indicating that fluorescence changes responded to $[\text{Ca}^{2+}]_i$ but not to pH_i .

Application of G-CaMP1.6 to Hippocampal Neurons. We also tested G-CaMP1.6 in rat hippocampal CA1 neurons, in which postsynaptic Ca^{2+} transients were evoked by stimulation of endogenous glutamate receptors. Hippocampal slices in which the G-CaMP1.6 cDNA was introduced were cultured at 35°C for 5 days. When the slices transferred to the recording chamber, the fluorescence was hard to see. However, we could easily identify fluorescent cells after waiting for ~ 30 min at 23 – 25°C . Figure 6 illustrates that application of $100 \mu\text{M}$ glutamate elicited a remarkable increase in fluorescence in the neuron expressing G-CaMP1.6. Notably, the fluorescence change of G-CaMP1.6 was observed not only at dendritic shafts but also at dendritic spines, the putative synaptic sites, in the G-CaMP1.6-expressing neuron. The extent of fluorescence change for G-CaMP1.6 was large enough to distinguish signals from noise in hippocampal slices.

DISCUSSION

In this work, we developed an additional fluorescent version of G-CaMP by introducing mutations in the cpEGFP part of G-CaMP. The new probe G-CaMP1.6 allowed us to easily monitor local Ca^{2+} changes in such tiny structures as dendritic spines of neurons. The brightness of G-CaMP1.6 is helpful to distinguish Ca^{2+} signals from noise when the cells have autofluorescence.

Until now, several mutations that enhance the GFP chromophore formation have been reported,²⁴ and they are categorized into two groups according to the location of their residues whether they are in the central α -helix (F64L, V68L, and S72A) or in outer β -sheets of GFP (Y145F, S147P, V163A, and I167T (pointing into the interior of GFP) and F99S, N146I, M153T, S175G, and N212K (facing outward of GFP)). It is not known, however, how these mutations contribute to improving the efficiency of GFP chromophore formation. According to crystallographic studies for GFP,²⁴ none of those listed residues of either group interacts directly with the chromophore. Among these mutations, some lead to an increase in extinction coefficient, and some lead to an increased chromophore formation at 37°C . Particularly, V163A and S175G have been reported to result in the increases in both the extinction coefficient and the increased chromophore formation at 37°C ; thus, these two mutations were tested to modify G-CaMP. Although V163A/S175G mutations did not facilitate the fluorescence development of the probe at 37°C , these mutations

(32) Dickson, R. M.; Cubitt, A. B.; Tsien, R. Y.; Moerner, W. E. *Nature* **1997**, *388*, 355–358.

enhanced the brightness of the probe by ~ 40 times. The change in brightness resulted from increases in both extinction coefficient and quantum yield (Table 1). It is notable that the quantum yield for G-CaMP1.6 was 0.79 in the presence of Ca^{2+} , this value being as large as that for EGFP.²⁴ This result may suggest that V163A/S175G mutations produced a more stable environment for the chromophore in G-CaMP1.6 than that in G-CaMP.

V163A/S175G mutations of G-CaMP1.6 also accelerated the rate of the fluorescence increase upon temperature change from 37 to 28 °C by ~ 3.5 times (Figure 3A and B). In addition, G-CaMP1.6 stayed sufficiently bright even at 37 °C for more than 20 h, once this probe was briefly exposed at a low temperature such as 28 °C (Figure 3E). Because of these properties, together with the brightness of G-CaMP1.6, $[\text{Ca}^{2+}]_i$ measurements in live cells with G-CaMP1.6 become easier to perform than those with G-CaMP. In fact, we could easily measure $[\text{Ca}^{2+}]_i$ changes even in tiny structures such as dendritic spines of hippocampal neurons (Figure 6).

Cubitt et al.³³ have proposed a sequential scheme for the chromophore formation of GFP, and Heim et al.³⁴ and Reid and Flynn³⁵ characterized the time constant for each step in the scheme using S65T-GFP. According to these reports, the rate-limiting step for the fluorescent chromophore formation is the final oxidation step. As for G-CaMP1.6, it is hard to know how fast the chromophore is formed under continuous exposure at 37 °C. Our results indicated that the quantum yield of G-CaMP1.6 decreased at 37 °C with little change in absorption and suggested that the rate-limiting step of G-CaMP1.6 for the fluorescence development upon temperature change from 37 to 28 °C is the maturation step of the proton network formation surrounding the G-CaMP1.6 chromophore.

As reported for wild-type GFP,²⁴ absorbance spectra for G-CaMP and its variants report the ionization status of the chromophore; i.e., the 400-nm peak and the 490-nm peak reflect neutralized (protonated) and ionized (deprotonated) states of the chromophore, respectively. Indeed, raising pH (from 7.5 to 10) increased ratios of ionized species to neutral species (Figure 1). In addition to the effect of alkalization, Ca^{2+} binding to these probes also enhanced chromophore ionization (Figure 1A–C and Table 1). As revealed by fluorescence excitation and emission spectra of G-CaMP variants (Figure 1D–F), excitation at ~ 400 nm failed to cause emission. Therefore, the increases in ratios of ionized species to neutral species in the presence of Ca^{2+} suggest that Ca^{2+} –CaM–M13 interactions produce effects on proton networks surrounding the chromophore, converting neutral species into ionized species. As shown in Table 1, Ca^{2+} increased the extinction coefficients at the 490-nm peak (the formation of ionized species) by 3.45 and 2.45 times for G-CaMP1.6 and G-CaMP, respectively. On the other hand, addition of Ca^{2+} also increased quantum yields of both G-CaMP1.6 and G-CaMP (~ 1.5 -fold each) (Table 1). Since fluorescence intensity (brightness) is proportional to the product of extinction coefficient and quantum yield, these data support that fluorescence intensities of G-CaMP1.6 and G-CaMP in the presence of Ca^{2+} were 4.9 and 4.5 times larger than those in the absence of Ca^{2+} , respectively.

Another point to be noted is that, even at a high pH (such as pH 10), fluorescence intensities of G-CaMP variants obtained in the presence of Ca^{2+} were 1.6–1.9 times higher than those in the presence of EGTA (data not shown). This result suggests that low proton and high Ca^{2+} concentrations have a synergistic effect on forming ionized species.

Other merit of using G-CaMP1.6 than its properties of bright fluorescence and fast fluorescence development is that it has smaller Hill coefficients for proton than G-CaMP both in the absence and in the presence of Ca^{2+} (Figure 2C,D and Table 1). Insensitivity to halides is also an advantage of using G-CaMP variants (Figure 2E–G). This feature is similar to that of EGFP,²⁴ a prototype GFP for G-CaMP variants. The Cl^- sensitivity of the fluorescence properties of a GFP variant named yellow fluorescent protein (YFP) may limit the usefulness of this chromophore as a Ca^{2+} probe in some cases. Moreover, several divalent cations (1 mM Ni^{2+} , Co^{2+} , Zn^{2+} , Mn^{2+} , Cd^{2+} , Sr^{2+} , and Ba^{2+}) caused fluorescence changes of G-CaMP variants to some extent (Figure 2H and I), though divalent cations that strongly affected fluorescence intensity were somehow different between G-CaMP and G-CaMP1.6. The effects of these cations are likely based on the fact that the EF hand structure in CaM shows some sensitivities to these cations at submillimolar concentrations.^{25,26} Although Mg^{2+} is a major concern to disturb signals of G-CaMP variants due to its presence at millimolar concentrations in cells, our present results indicate that Mg^{2+} does not affect the fluorescence intensity of G-CaMP variants. Ba^{2+} and Sr^{2+} had much lower affinities than Ca^{2+} , showing that these cations are also less likely to affect fluorescence intensities of G-CaMP variants in physiological conditions. Cations having an ionic radius similar to Ca^{2+} (0.100 nm) were reported to potentially induce structural changes in CaM²⁵ and to affect interactions of CaM with its target peptides.²⁶ No strong correlation, however, was observed between the ionic radius of divalent cations and fluorescence intensity of G-CaMP. On the other hand, we found that G-CaMP1.6 was more selective than G-CaMP to divalent cations having an ionic radius similar to Ca^{2+} , indicating that G-CaMP1.6 is a better Ca^{2+} probe than G-CaMP. Since mutations introduced into G-CaMP1.6 are located only in the GFP part of the probe, we speculate that the fusion of CaM with cpEGFP in G-CaMP variants induce minute structural changes at EF hands of CaM, which might be enough to affect binding of divalent cations. It might be possible that the slight structural change in CaM of G-CaMP and G-CaMP1.6 affects the relationship between the ionic radius of divalent cations and fluorescence changes. If this is the case, CaM in G-CaMP might have more structural stress than that in G-CaMP1.6.

We introduced mutations at the Z(–) coordination position of each EF hand of CaM (E31K, E67K, E104K, and E140K) in G-CaMP1.6 to change its affinity for Ca^{2+} and to reduce its Ca^{2+} -buffering effect. Among the CaM variants of G-CaMP1.6, G-CaMP1.6–CaM(E140K) seems the most useful for monitoring $[\text{Ca}^{2+}]_i$, because it possesses properties similar to those of G-CaMP1.6: high extinction coefficient, high quantum yield, high affinity for Ca^{2+} at the range of $[\text{Ca}^{2+}]_i$, mild affinity for proton, and large fluorescence change in response to Ca^{2+} (Table 1). Besides, since the Ca^{2+} -buffering effect of G-CaMP1.6–CaM(E140K) is presumably smaller than that of G-CaMP1.6, G-CaMP1.6–CaM(E140K) should have less effect on native Ca^{2+}

(33) Cubitt, A. B.; Heim, R.; Adams, S. R.; Boyd, A. E.; Gross, L. A.; Tsien, R. Y. *Trends Biochem. Sci.* **1995**, *20*, 448–455.

(34) Heim, R.; Cubitt, A. B.; Tsien, R. Y. *Nature* **1995**, *373*, 663–664.

(35) Reid, B. G.; Flynn, G. C. *Biochemistry* **1997**, *36*, 6786–6791.

signals, when expressed in cells. Surprisingly, glutamate-to-lysine mutations in the CaM part currently performed did not shift the affinity for Ca^{2+} binding of G-CaMP1.6 so dramatically. In addition to combination of these mutations, replacing the target peptide of CaM (the M13 fragment of myosin light chain kinase) with a peptide that shows a different affinity for binding to CaM (e.g., a peptide derived from type I adenylylcyclase,^{29,36–38} which shows lower affinity for CaM by ~ 150 times) may provide an alternate means of shifting probe affinity for Ca^{2+} .

CONCLUSION

G-CaMP1.6 is an improved genetically encoded probe suitable for imaging $[\text{Ca}^{2+}]_i$ fluctuations at submicromolar concentrations.

(36) Klee, C. B.; Crouch, T. H.; Richman, P. G. *Annu. Rev. Biochem.* **1980**, *49*, 489–515.

(37) Huang, S.; Carlson, G. M.; Cheung, W. Y. *J. Biol. Chem.* **1994**, *269*, 7631–7638.

(38) Brown, S. E.; Martin, S. R.; Bayley, P. M. *J. Biol. Chem.* **1997**, *272*, 3389–3397.

Since G-CaMP1.6 exhibits increased green fluorescence and rapid fluorescence development, this new Ca^{2+} probe will provide a more practical alternative than G-CaMP for experiments particularly to monitor local Ca^{2+} changes in tiny structures such as dendritic spines of neurons.

ACKNOWLEDGMENT

We thank Seiko Miura and Mitsutoshi Ono for technical assistance. We also thank Dr. Robert Dirksen for reading the manuscript. This work was partly supported by grants from the Ministry of Education, Culture, Sports, Science and Technology in Japan, and from the Japan Society for the Promotion of Science.

Received for review April 20, 2005. Accepted July 11, 2005.

AC0506837